Available online at www.sciencedirect.com

ScienceDirect

Procedia Engineering 147 (2016) 348 – 353

Procedia Engineering

www.elsevier.com/locate/procedia

11th conference of the International Sports Engineering Association, ISEA 2016

Non linearity of the ball/rubber impact in table tennis: experiments and modeling

Renaud G. Rinaldi[a,*], Lionel Manin[b], Clément Bonnard[b], Adeline Drillon[b], Hugo Lourenco[c], Nicolas Havard[c]

[a]*Université de Lyon, INSA-Lyon, MATEIS UMR 5521, F-69621 Villeurbanne France*
[b]*Université de Lyon, INSA-Lyon, LaMCoS UMR 5259, F-69621 Villeurbanne France*
[c]*Cornilleau, Bonneuil-Les-Eaux, 60121 Breteuil France*

Abstract

Along with *comfort*, the *speed* is a key metric used to qualify the performance of a table tennis racket. The restitution coefficient which corresponds to the ratio between the velocities of the ball right before and after normally impacting the racket relates to the speed performance: the higher the restitution coefficient, the greater the *speed*. Thus, understanding the normal impact problem is key and suggests investigating the effects of the intrinsic properties and architectures of the constituents of the racket. In this work, both experimental and numerical studies were pursued. Experimentally, normal impact tests were performed for varying launching velocities on samples made of isolated or associated constituents of a table tennis racket and the restitution coefficients calculated. Numerically, 3D finite elements simulations were conducted to replicate the normal impact conditions while incorporating the time-dependent constitutive behavior of the polymeric elements contributing during the impact: the racket constituents (the foam and the compact) and the ball. The restitution coefficients are seen to decrease with increasing launching velocity, while being minimum when the two racket polymeric constituents are associated. A fair agreement is obtained with the FE simulations in which the sample/ball contact zone is identified as a ring with its mean radius increasing till the maximum crushing. Ultimately, additional FE calculations confirm that the friction plays a key role in the energy dissipation process, alongside with the rate-dependent behavior and architecture of the polymeric constituents.

Peer-review under responsibility of the organizing committee of ISEA 2016
Keywords: normal impact; restitution coefficients; polymers; architecture; energy dissipation

1. Introduction

A table tennis racket is a complex layered hybrid materials comprising two polymeric sheets glued on to a wooden blade: an elastomeric dense foam and an architectured rubber (comprising a regular array of small cylinders) so-called compact. When impacted by a ball, both polymeric constituents can exhibit large reversible yet dissipative deformation, playing a key role in preserving the ball from breaking as well as contributing to the comfort and speed performances of the racket. Thus, manufacturers need to account for the polymeric constituents' properties and geometries in order to enhance the performances of new products.

Normal impact tests and the determination of the coefficient of restitution are used to evaluate the speed, which is the performance of interest in this study. Little is reported on the complex behavior of the racket constituents and their responses when normally impacted by a ball. However, the normal crushing of a thin-wall spherical launcher on a flat rigid surface has been widely studied. Quasi-static and/or dynamic behavior evidenced the buckling of the thin-wall sphere [1-5]. In studies where a table tennis ball is used, the celluloid constitutive materials is sometimes described as an elastic perfectly plastic material [1] even though glassy polymeric materials are complex viscoelasto-viscoplastic materials [6, 7]. Thus, the celluloid rate-sensitivity needs to be accounted

* Corresponding author. Tel.: +33-4-72-43-62-09; fax: +33-4-72-43-85-28
E-mail address: renaud.rinaldi@insa-lyon.fr

Peer-review under responsibility of the organizing committee of ISEA 2016
doi:10.1016/j.proeng.2016.06.307

for, specifically when the impact problem is considered and the properties measured under quasi-static conditions [4, 5]. Indeed, under dynamic conditions, the modulus and yield strength increase compared to low rate values. Recently, Zhang *et al.* used an inverse-fitting method to describe the visco-elastic properties of the celluloid material and to model the impact of a table tennis ball impacting a rigid surface [8].

Thus, the measurements of the visco-elastic properties of the ball is a real need and naturally, in the current problem where the rigid target can be replaced by polymeric ones, a precise description of the dissipative rate-dependent properties of the other polymeric counterparts are crucial. Thus, along with a precise account for the layers architecture, this work aims towards the identification of the key factors/effects altering the overall speed performance of a commercially available table tennis racket coating comprising a foam layer and a compact layer.

Nomenclature

${}^{R}C_R$, ${}^{F}C_R$, ${}^{FC}C_R$,	Coefficient of Restitution when the ball impacts a rigid, a foam or a foam+compact target respectively (-).
V_i , V_R	Incident and Reflected velocities respectively (m/s).
${}^{B}T_g$, ${}^{F}T_g$, ${}^{C}T_g$	Glass Transition Temperature of the ball, the foam and the compact respectively (°C).
ρ, ϱ	Absolute (kg/m^3) and relative (-) densities.
${}^{C}\nu$, ${}^{F}\nu$	Poisson ratio of the compact and the foam respectively (-)
DMA	Dynamic Mechanical Analysis.
DSC	Differential scanning Calorimetry.
FE	Finite Element

2. Normal impact experiments

2.1. Samples preparation

A commercial product from Cornilleau© is investigated. Xylene solvent was used to separate the foam layer from the compact layer. 100 mm x 100 mm squares of the foam and the foam+compact were cut, measured and weighted to determine their absolute densities (ρ) and glued onto rigid plates using double-sided adhesive tape. The balls were also measured and weighted to prevent abnormality.

2.2. Set-up and protocol

A home-made apparatus has been designed to launch table tennis balls yet controlling the ball's initial velocity and spin. The target is fixed normal to ball's trajectory onto the rigid frame, 260 mm away from the launcher's end. A camera coupled with stroboscopic lighting is set to acquire pictures which display the target as well as numerous traces of the ball before and after impact. Marks are drawn onto the target to locate its center and onto the ball to ascertain negligible spin and locate the joint equator. Two examples of recorded pictures are provided in Fig. 1a&b with clear identification of the drawn marks.

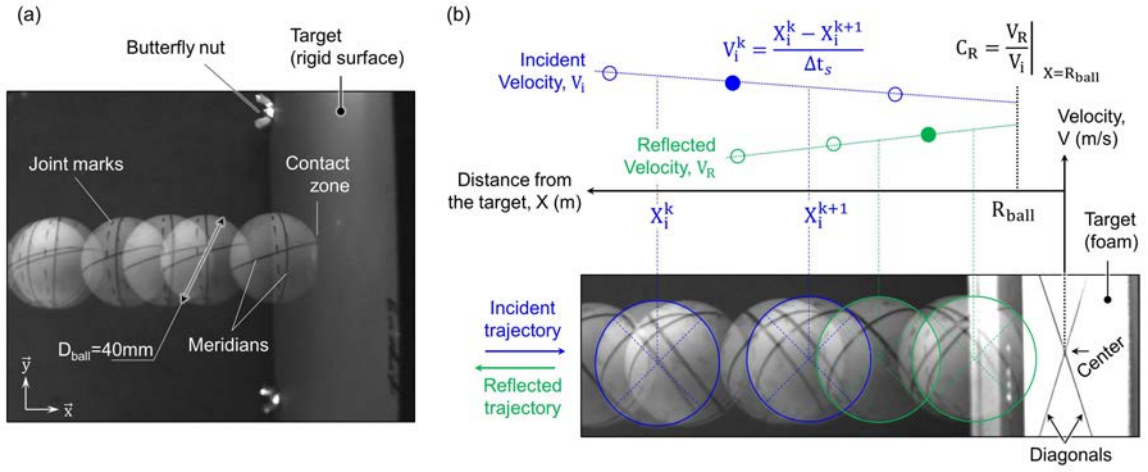

Fig. 1. Experimental determination of the restitution coefficient C_R: (a) raw image showing traces of the ball before, during and after contact with the rigid surface, (b) incident and reflected velocities are determined for different positions with respect to the impact location and extrapolated to determine the coefficient of restitution.

Using the aforementioned setup, normal impact experiments were performed at room temperature for launching velocities ranging from 5 to 30 m/s, consistent with the speed of the ball in game conditions. Twenty consecutive impacts were repeated for a given set of *{target; launching velocity}*. The first ten shots aimed at "warming up" the ball and the target materials. Out of the last ten shots, three pictures were visually selected so that:

- The ball spin was negligible: spin would cause noticeable deviation of the meridional marks drawn on the ball between two consecutive traces.
- The impact was normal: in the *xy*-plan of the pictures, this is confirmed when all the traces of the ball lie on a unique straight line. Now considering a potential tilt perpendicular to the picture, the perspective would cause the ball's size to decrease or increase as it moves away from the camera or towards the camera respectively.
- The contact zone did not contain the joint of the ball: this is ascertained by locating the dashed-line disk almost perpendicular to the ball's trajectory.

2.3. Metric of interest: Coefficient of Restitution

With the aid of the remaining filtered pictures, the coefficient of restitution was calculated following the procedure depicted in Fig. 1b and detailed hereafter: incident and reflected traces of the ball were separated assuming that the distance will be lower for two successive reflected traces compared to two successive incident ones. The centers of the ball's traces were then calculated by means of the image processing free software ImageJ©. Using the $\{x_c,y_c\}$ coordinates of two consecutive centers, the ball velocity was determined with respect to its position from the target ($x_{target}=0$), knowing that subsequent traces are separated by a time increment $\Delta t_s=1/f_s$ with f_s the stroboscopic frequency. Finally, the coefficient of restitution is set equal to the ratio between the incident and reflected velocities extrapolated right before contact and right after separation respectively, *i.e.* when the center x-coordinate x_c of the ball is a radius R_{ball} away from the target x_{target}.

The experimental coefficient of restitutions are presented in Fig. 2a as a function of the incident velocity. Within the range of velocity covered, the coefficients are seen to decrease with increasing incident velocity. They span from about 0.9 at 10 m/s down to about 0.4 around 30 m/s. For a given incident velocity, the coefficients of restitution of the three targets rank as follow ${}^{R}C_R > {}^{F}C_R > {}^{FC}C_R$ (the subscripts *R*, *F* and *FC* refer to the rigid, the foam and the foam+compact targets respectively) noticing that the difference between the foam layer and the foam+compact layer tends to diminish at low (10 m/s) and high (30 m/s) velocities. Lastly, it is worth noting that the normal impact of table tennis balls onto a rigid surface has been studied already and results with similar trend and values reported [8].

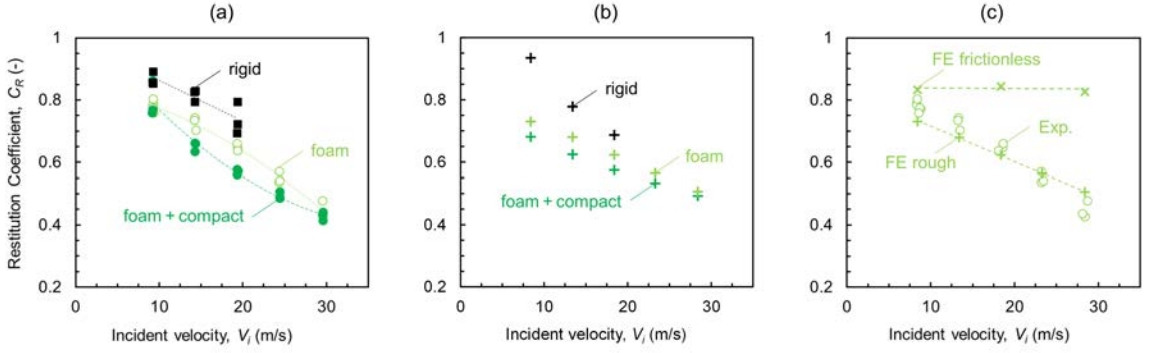

Fig. 2. Restitution coefficients as a function of the incident velocity: (a) experimental results (T=22±1 °C), (b) Finite Elements results, (c) effect of the ball/foam surfaces contact properties on the F.E. results and direct comparison with the experimental measurements.

3. Numerical models

Explicit 3D Finite Elements simulations using the commercial software ABAQUS© [9] are performed to model the normal impact problem and deduce the restitution coefficient with account for the geometry/architecture and the complex constitutive equations of the polymeric parts. The objectives of the numerical modeling is then twofold: first, simulations are pursued to identify the predominant phenomena taking place during the impact, and second to explore the effect of geometries. Details on the materials properties and the FE model are provided in the following paragraphs.

3.1. Mechanical behavior of the polymeric constituents

The number of polymeric elements varies from one (the ball) to three (the ball, the foam and the compact) depending on the target considered, rigid or foam+compact respectively. DSC measurements of the glass transition temperature confirmed that the

ball stands in its glassy regime ($^{B}T_g \approx 94$ °C$>T_{amb}$) while the foam and the compact are rubbery ($^{F}T_g \approx {}^{C}T_g \approx -60$ °C$<T_{amb}$) at room temperature. As already mentioned, glassy polymers exhibit complex non-linear viscoelasto-viscoplastic behavior. However, the ball maintains its original shape right after impact so that only its viscoelastic response is implemented hereafter. Rubbery materials are compliant and often described as rate-independent hyperelastic materials. Nevertheless, when tested at high velocity, they can transition into their leathery regime coinciding with an increase of its storage and dissipative moduli [10]. Consequently, during impact, both the large strain hyperelastic property and the viscoelastic property need to be modeled.

The viscoelastic behavior was measured through dynamic mechanical analysis (DMA). The specimens were tested in a EPLEXOR© apparatus by forced oscillatory loading at frequencies of 1, 5 and 25 Hz, over a temperature range of -50 to 75 °C, with heating rates of 1 °C/min. For the foam and the ball, small stripes were prepared and loaded in tension. For the compact, the intrinsic behavior could not be obtained because of its complex architecture. Thus, through-thickness 10 mm-diameter cylinders of the foam+compact were punched and the viscoelastic properties of the "Reuss (series) composite" tested in compression. The DMA measurements are reported in Fig. 3a&b where the storage modulus and loss factor, also known as the material damping factor, are reported versus temperature. Fig. 3a displays the foam behavior for the three frequencies. At room temperature, the foam stands in its rubbery regime with low modulus and damping. Both modulus and damping increase with decreasing temperature as the system enters its leathery regime coinciding with the high temperature regime of the main relaxation (often assimilated to the glass transition temperature). This transition is shifted towards high temperature with increasing frequency emphasizing the thermo-rheological simplicity of the material [11]. In Fig. 3b, the 1 Hz isochronal responses of the ball, the foam and the foam+compact are superimposed. Within the temperature range covered, the ball exhibits high modulus, of the order of 2 GPa consistent with measurements reported in the literature [1, 5], and moderate damping (less than 0.1). Interestingly, the foam and foam+compact profiles are very similar, so that the foam viscoelastic behavior will be used for both polymeric constituents in the remaining.

For the large strain response, a quasi-static compression test was carried out on a Zwick mechanical testing machine at ambient temperature (22±1°C) and constant crosshead speed, *i.e.* constant nominal strain rate of 10^{-3} /s. Foam cylinder with an aspect ratio (length / diameter) of about 1 were punched out of the 2 mm thick foam sheet. The non-linear nominal stress–nominal strain profile up to 70% compression strain is presented in Fig. 3c.

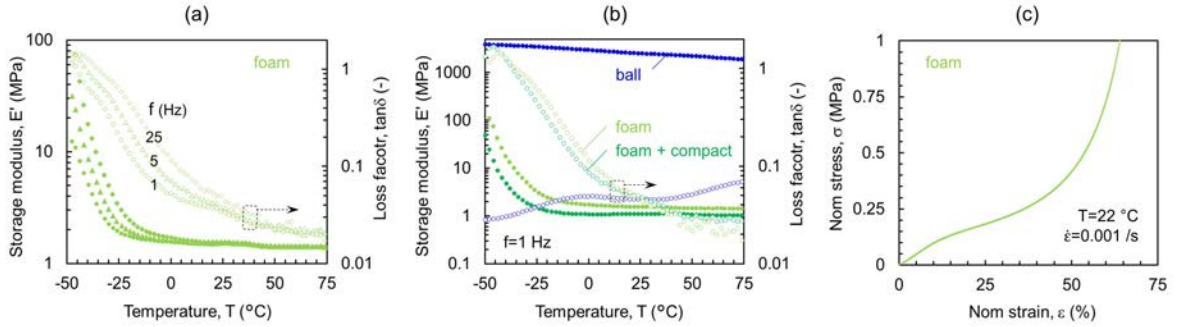

Fig. 3. Experimental measurements of the mechanical behavior of the polymeric constituents: (a, b) DMA measurements of the viscoelastic behavior, (c) large strain compressive response of the foam layer.

In ABAQUS©, Prony series, also known as generalized Maxwell model, are used to model the time-dependent shear modulus of visco-elastic materials $G(t)$. A detailed presentation of the theory and the parameters to be entered can be found in [8]. The time-dependent shear modulus profile is obtained from the DMA measurements following the procedure depicted in [12] and based on the thermo-rheological simplicity. Nine discrete Maxwell elements were identified for the ball and the foam. Constant Poisson ratio are allocated to the polymeric constituents to control the volumetric behavior. Table data of the experimental strain-stress profile is used for the long-time large strain behavior.

As evoked above, the viscoelastic and large strain properties of the foam determined experimentally are assigned to the foam and the compact constituents. Two important differences remain: the foam being modeled as a continuum media, its density and Poisson ratio must differ from the compact for which the exact architecture is modeled. Consequently, almost incompressible Poisson ratio ($^{C}\nu$=0.49) and density ($^{C}\rho$=1000 kg/m^3) of the parent materials need to be documented for the compact whereas effective values are required for the foam: $^{F}\rho$=490 kg/m^3 (dimension and weight measurements) and $^{F}\nu$=0.41 (determined using video-extensometry). It is worth noting that the Poisson ratio of low density foams tends towards 0 with decreasing relative density [13] so that the HYPERFOAM model is usually employed to mimic the large strain response of these systems. In our case, the relative density of the foam is too high ($^{F}\rho \approx 0.44$ measured using X-ray tomography) so that the HYPERELASTIC description is preferred.

The 3D FE model of the ball normally impacting the foam+compact target and figuring the converged mesh and key dimensions is displayed in Fig. 4a&b. Shell elements SR4 with five integration points through the thickness are used for modeling the ball, C3D8R elements are used for the foam and the compact, and the rigid target is defined as a rigid body. The bottom surface of the target is fixed and the ball impacts it with a velocity V_i. The contact between the two bodies is defined rough if not otherwise

specified. Rough contact condition prevails since simulations did not evidence major discrepancy with simulations where the penalty method with the friction coefficient $\mu \approx 2$ was used (see [14] for experimental measurements of the friction coefficient). Lastly, constant internal pressure is prescribed as justified elsewhere [8].

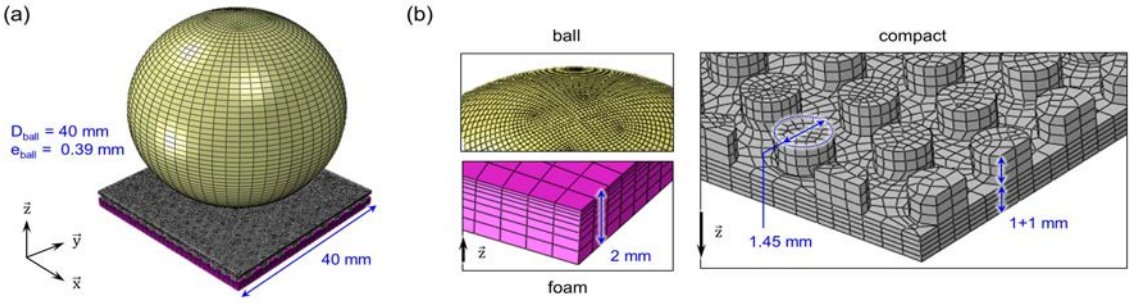

Fig. 4. (a) 3D finite elements model, (b) close-up views of the converged meshes for the 3 parts: the ball, the foam and the compact.

4. Results

4.1. Prediction of the restitution coefficient

The predicted coefficients of restitution are presented in Fig. 2b right next to the experimental data (Fig. 2a) The numerical results show good agreement with the experimental data: the predicted coefficients of restitution decrease with increasing incident velocity and the energy dissipation is maximum for the foam+compact target and minimum for the rigid target. A direct comparison between the experimental and predicted restitution coefficients of the foam is reported in Fig. 2c where the contact property between the foam and the ball is changed from rough to frictionless. A clear deviation between the experimental and simulated data is observed when the contact is considered without friction. Furthermore, frictionless simulations tend to over predict the experimental measurements and do not seem to evolve with speed so that the discrepancy between the experiments and the simulations increases with increasing velocity. Ultimately, an important cause of energy dissipation comes from the friction process. This major role can be explained by the sample/ball contact zone which is identified as a ring with its mean radius increasing till the maximum crushing. The ball buckling phenomena has been largely studied and reported in the literature [8], observed experimentally in this work (see the contact zone in Fig. 1a) and simulated numerically (see Fig. 5a&b). The greater the incident velocity, the larger the maximum radius of the ring and the more important the friction dissipation is.

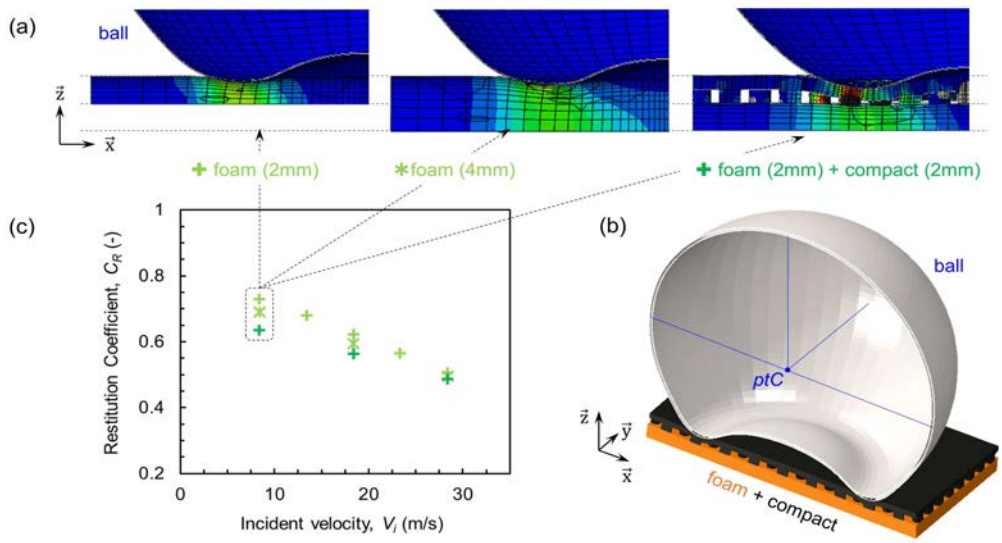

Fig. 5. Effect of architecture: (a) Deformation profiles for V_{ptC} =0 m/s (the color contours represent the through thickness true stress component σ_{ZZ}, (b) isometric view of half the ball impacting the foam+compact for V_{ptC} =0 m/s, (c) restitution coefficients as a function of the incident velocity.

4.2. Effect of architecture

Assigning the same constitutive equations to the foam and the compact is pertinent when looking at the DMA measurements presented in Fig. 3b. Besides, it permits to study of the effect of the targets architecture. This is done by predicting the restitution coefficients of three targets: a 2 mm thick foam, a 4 mm thick foam and a 2+2 mm thick foam+compact. The results are summarized in Fig. 5. Fig. 5a&b display the contact zones at maximum crushing. The differences between the foams of varying thickness is little, whereas the foam+contact system exhibit augmented through-thickness crushing, mostly in the compact layer. The cylinders of the compact right beneath the contact ring reveal severe through-thickness crushing. The contact surface area is thus increased, suggesting more dissipation through friction. The restitution coefficients plotted in figure 4c as a function of the impacting velocity show quantitative differences between the three systems. While the C_R seem to merge for high velocity, the 2+2 mm foam+compact systems dissipates the most, which is consistent with the aforementioned hypothesis.

5. Conclusions

The present study focuses on the effect of the polymeric coatings on the speed performance of a tennis table racket. The metric of interest is the coefficient of restitution of a ball normally impacting the targets under study. Both experimental and numerical efforts were pursued. The precise architecture and the viscoelastic yet dissipative properties of the polymeric layers have been implemented. A fair comparison is obtained between the experimental data and FE predictions showing that the restitution coefficient decrease with the increase of the ball incident velocity. The elastic buckling of the ball during normal impact is evidenced and leads to a radially growing ring contact surface. Ultimately, the peculiar contact implies that the friction between the ball and the target(s) is a major source for energy dissipation, as confirmed numerically. Additionally, the compliance of the rubbery coatings, which in turn depends on its architecture, also triggers the contact surface and thus the balance between materials and contact energy dissipations and the resulting speed performance.

Recently, a python script for ABAQUS© has been developed to greatly enhance the versatility of the numerical tool by rapidly varying the targets architecture and/or the materials intrinsic properties. Consequently, extensive studies are pursued to identify the optimized configurations (in terms of both geometries and material properties) towards enhanced speed performance.

References

[1] Ruan HH, Gao ZY, Yu TX. Crushing of thin-walled spheres and sphere arrays. Int J Mech Sci 2006;48:117-133.
[2] Shorter R, Smith JD, Coveney VA, Busfield JJC. Axial compression of hollow elastic spheres. J Mech Mat Struc 2010;5(5): 693-705.
[3] Pauchard L, Rica S. Contact and compression of elastic spherical shells: the physics of a ‘ping-pong’ ball. Philos Mag B 2010;78(2): 225-233.
[4] Zhang XW, Tao Z, Zhang QM. Experimental and Numerical Study on the Dynamic Buckling of Ping-pong Balls under Impact Loading. Int J Nonlinear Sci Numer Simul 2012;13:81-92.
[5] Dong XL, Gao ZY, Yu TX. Dynamic crushing of thin-walled spheres: An experimental study. Int J Impact Eng 2008;35:717-726.
[6] Rinaldi R, Gaertner R, Chazeau L, Gauthier C. Modeling of the mechanical behavior of amorphous glassy polymer based on the quasi-point defect theory—Part I: Uniaxial validation on polycarbonate. Int J Non-Lin Mech 2011;46(3):496-506.
[7] Rinaldi R, Gaertner R, Brunet M, Chazeau L, Vidal-Sallé E, Gauthier C. Modeling of the mechanical behavior of amorphous glassy polymer based on the quasi-point defect theory—Part II: 3D formulation and finite element modeling of polycarbonate. Int J Non-Lin Mech 2011;46(3):507-518.
[8] Zhang XW, Tao Z, Zhang QM. Dynamic behaviors of visco-elastic thin-walled spherical shells impact onto a rigid plate. Latin Amer J Solids Struc 2014;9(27):2607-2623.
[9] Abaqus: http://www.3ds.com/products-services/simulia/products/abaqus/
[10] Rinaldi RG, Hsieh AJ, Boyce MC. Tunable microstructures and mechanical deformation in transparent poly(urethane urea)s. J Polym Sci PartB: Polym Phys 2011;49(2):123-135.
[11] Lakes R. Viscoelastic materials. Cambridge University Press; 2009.
[12] Cho H, Rinaldi RG, Boyce MC. Constitutive modeling of the rate-dependent resilient and dissipative large deformation behavior of a segmented copolymer polyurea. Soft Matter 2013;9(27):6319-6330.
[13] Gibson LJ, Ashby MF Cellular solids: structure and properties. Cambridge university press; 1997.
[14] Varenberg M, Varenberg A. Table Tennis Rubber: Tribological Characterization. Tribol Lett 2012;47:51–56.